Proceedings World Geothermal Congress 2000
Kyushu - Tohoku, Japan, May 28 - June 10, 2000

A FULLY THREE-DIMENSIONAL THERMO-HYDRAULIC COMPUTATION OF THE OGACHI HDR RESERVOIR

Hiroshi SUENAGA* Takeshi YAMAMOTO* Yuzuru EGUCHI* Koichi KITANO*
Hiroshi OHNISHI**

*The Central Research Institute of Electric Power Industry (CRIEPI)
** Denryoku Computing Center (DCC)
1646 Abiko, Abiko-shi, Chiba, JAPAN 270-1194

Key Words: HDR, Darcy model, reservoir analysis, finite volume method, Ogachi

ABSTRACT

A fully three-dimensional simulation code, GEOTH3D, is developed to solve thermo-hydraulic features of a Hot Dry Rock(HDR) geothermal reservoir. The objectives of the code development are to help understand experimental data obtained in the CRIEPI's Ogachi HDR site, and optimize design of a planned HDR system by predicting thermal and hydraulic performances. Unique aspect of the GEOTH3D is that the reservoir structure is modeled by porous media of spatially variable permeabilities which are determined with aid of acoustic emission(AE) measurements at an HDR site and local permeability measurement around the wells. Based on the permeability distribution, the GEOTH3D code computes the 3D distribution of Darcy velocity, pressure and temperature, including the interaction between flow and temperature, but not the effects of rock stress and flow apertures.

For validation, the GEOTH3D code was applied to a thirty day circulation test conducted at the Ogachi site in 1995, using time-dependent pressures at the injection and the production well heads. The temporal changes of the injection and production flow rates are compared with actual rates to quantitatively evaluate the applicability of the code. As a result, the computed flow rates approximately corresponded to the measured rates.

1. INTRODUCTION

A computer code to simulate thermo-hydraulic behavior in an HDR reservoir, GEOTH3D, has been developed in the CRIEPI. The objectives of the code development are to help understand experimental data obtained in the CRIEPI's Ogachi HDR site, and to apply to design optimization of a planned HDR system by predicting thermal and hydraulic performances. The GEOTH3D code computes a 3-D distribution of Darcy velocity, pressure and temperature, including the interaction between flow and temperature, but not the effects of rock stress and deformation on apertures. A feature of the GEOTH3D is that permeability distribution of a reservoir is estimated using AE measurement at an HDR site and local permeability measurement around the wells(Y. Yamamoto et al.,1996). That is, the GEOTH3D takes account of a reservoir structure in the numerical model.

Since the original GEOTH3D code lacked computational robustness, i.e., numerical convergence and applicability to various operational conditions of a real HDR site, parts of the present authors (Y. Eguchi *et al.*, 1998) have restructured the GEOTH3D code by replacing the original two-phase flow formulation with a single-phase flow formulation, and by introducing pressure-prescribed boundary conditions instead of the flow-rate boundary condition. The modified code can do matrix-inversion iteration without numerically instability and rapid convergence, yielding reliable solutions.

In the present study, the GEOTH3D code is applied to a thirty day circulation test conducted at the Ogachi site in 1995, given time-dependent pressures at the injection and the production well heads. The temporal changes of the injection and production flow rates and temperature will be compared with those of the Ogachi measurement to quantitatively evaluate the applicability of the code.

In the following section, the GEOTH3D code is outlined including the basic equations and boundary conditions. The permeability model is explained in Section 3. In Section 4, computational results for 1995 Ogachi experiment are presented to evaluate hydraulic behavior.

2. OUTLINE OF GEOTH3D

2.1 Basic equation

The basic equations employed in the GEOTH3D are based upon the following assumptions.

1. Fractured rock is expressed by porous media approximation, while flow through rock matrix is subject to the Darcy's law.
2. State of water is always liquid-phase.
3. Physical properties such as density and viscosity of water are independent of temperature, since energy equation is not considered so far in the present study solely to see how the code works for velocity (or recovery) and pressure computation.
4. Density of water, ρ_w, and porosity of rock, ϕ, are linear functions of pressure as follows.

$$\rho_w = \rho_0\{1 + \beta_w(p - p_0)\} \quad (1)$$
$$\phi = \phi_0 + (1 - \phi_0)\beta_r(p - p_0) \quad (2)$$

where β_w and β_r are pressure compressibility coefficients for water and rock, respectively. Subscript '0' stands for a reference value at $p = p_0$.

With the above assumptions, the followings are obtained as the basic equations, using Darcy velocity, $\vec{u}$, and pressure extracting hydrostatic pressure, p , as primary variables.

Darcy's law :

$$\vec{u} = -\frac{k}{\eta}\nabla p \quad (3)$$

Mass conservation law :

$$m_{,t} = -\rho_0 \nabla^T \cdot \vec{u} + q \quad (4)$$

The mass of water per unit volume, m, is defined by the product of water density, ρ_w, and rock porosity, ϕ, being approximated as follows.

$$\begin{aligned} m &= \rho_w \phi \\ &= \rho_0\{1 + \beta_w(p - p_0)\}\{\phi_0 + (1 - \phi_0)\beta_r(p - p_0)\} \\ &\approx \rho_0\phi_0 + \rho_0\{\phi_0\beta_w + (1 - \phi_0)\beta_r\}(p - p_0) \end{aligned} \quad (5)$$

2.2 Boundary conditions

In general, total flow rate at an injection well is under our control during circulation tests and can be used as a boundary condition. However, a total flow rate at the production well is generally unknown a priori and then can not be used as a boundary condition. Furthermore, it is very difficult in practice to measure flow rate distribution along whole open interval of both injection and production well bores. Especially the Ogachi site is the case, since there are two major flow paths from the injection well to the production well because of the double major fracture zones.

Then, pressures along open hole intervals of production and injection wells are fixed as boundary conditions to supplement the basic equations, eqs. (3) and (4). Pressure can be set at hydrostatic pressure along the well bores, also on outmost computational boundary.

$$p(t) = p^{IN}(t) \text{ in an inj. wellbore} \quad (6\text{-a})$$
$$p(t) = p^{PRO}(t) \text{ in a prod. wellbore} \quad (6\text{-b})$$
$$p(t) = 0 \text{ on outmost boundary} \quad (6\text{-c})$$

where $p^{IN}(t)$ and $p^{PRO}(t)$ are time-series of pressures measured at the injection well head and at the production well head, respectively.

2.3 Computational discretization

Finite volume discretization was applied to eqs. (3) and (4) in three-dimensional spatial domain, substituting eq.(5) into eq.(4) to yield the following linear algebraic equations.

Discretized Darcy's law:

$$\vec{U} = -\frac{k}{\eta}[C]\vec{P} \quad (7)$$

$$\rho_0\beta\vec{P}_{,t} = -\rho_0[C]^T\vec{U} + \vec{Q} \quad (8)$$

where $\vec{U}$, $\vec{P}$ and $\vec{Q}$ are vectors of discretized velocities, discretized pressures and discretized flow source/sink, respectively, while Matrix [C] is derived from gradient operator, ∇. The total compressibility coefficient, β, is expressed as follows.

$$\beta = \phi_0\beta_w + (1 - \phi 0)\beta_r \quad (9)$$

Combining eqs.(7) and (8), the following pressure Poisson equation is obtained in a discrete form.

$$\rho_0\beta\vec{P}_{,t} = \frac{\rho_0 k}{\eta}[C]^T[C]\vec{P} + \vec{Q} \quad (10)$$

The descretized form of the pressure-prescribed boundary conditions is given as follows.

$$P_{ijk}(t) = p^{IN}(t) - \Delta p^{IN^*} \quad (11\text{-a})$$
$$P_{ijk}(t) = p^{PRO}(t) + \Delta p^{PRO^{**}} \quad (11\text{-b})$$
$$P_{ijk}(t) = 0^{***} \quad (11\text{-c})$$

*at inj. well grids
**at prod. well grids
***on outmost boundary

where Δp^{IN} and Δp^{PRO} represent pressure drop within a pressure-prescribed grid around the injection well and the production well, respectively. The estimate is explained in the following subsection.

If the steady-state is of interest, left-hand side term of eq. (10) can be droped and solved with steady-state pressure boundary conditions.

2.4 Difference of grid-averaged pressure and well bore pressure

Because a grid scale is mostly much larger than a diameter of well bore, and because pressure gradually decays (for an injection well) or increases (for a production well) along the distance from the well, prescription of pressure at a whole grid can cause deviation from the real situation. Therefore, in the following, the deviation is quantified for an axis-symmetric permeating flow in a uniform porous media, where the steady-state radial Darcy velocity, u_r, can be written as follows.

$$u_r = -\frac{k}{\eta}\frac{\partial p}{\partial r} \tag{12}$$

The total flow rate, Q_0(positive for inflow; negative for outflow), through a cylindrical surface of radius, r, and the vertical interval, L, is given by the following, using the above relations.

$$Q_0 = -2\pi r L u_r = \frac{2\pi r L k}{\eta}\frac{\partial p}{\partial r} \tag{13}$$

Integration of the above equality gives the following relation.

$$p - p_{well} = G \ln \frac{r}{r_w} \qquad (r \geq r_w) \tag{14-a}$$

$$p = p_{well} \qquad (r_w \geq r \geq 0) \tag{14-b}$$

where G represents $\frac{Q_0 \eta}{2\pi L k}$. Assuming a cubic computational grid can be represented by a cylinder of radius, R, the volume-averaged pressure within the cylinder, p, is calculated as follows.

$$\begin{aligned} \underline{p} &= \frac{\int_{r_w}^{R} p \cdot 2\pi r dr}{\int_{r_w}^{R} 2\pi r dr} \\ &= G\frac{\alpha^2 \ln \alpha}{\alpha^2 - 1} + p_{well} \end{aligned} \tag{15}$$

where α is the ratio of grid radius, R, to well radius, r_w, i.e., $\frac{R}{r_w}$. Since the length of unit grid is $20m$ in the present study, the equivalent grid radius, R, may be given by the equal-area-relation, $\pi R^2 = 20^2$. Then, the difference between the averaged pressure within a grid and well pressure, $\underline{p}$ - p_{well} (i.e., $-\Delta p^{IN}$ or Δp^{PRO}) is calculated *via* eq. (15) based on the data measured at the Ogachi site in the '95 thirty-day circulation test, and the results are tabulated in Table 1.

As seen in Table 1, there is a difference of $1.2MPa$ between the grid-averaged pressure and the well pressure at the injection well under a steady-state condition, though the pressure for the production interval will be in good agreement with the grid-averaged pressure.

2.5 Flow rate computation

The flow rates at both an injection well and a production well, Q_0, are not needed specifying, but naturally calculated *via* surface integration of computed velocity around each well as follows.

$$\begin{aligned} Q_0 &= \sum_{k=1}^{K} U_k \Delta y_k \Delta z_k \delta_k \\ &+ \sum_{m=1}^{M} V_m \Delta z_m \Delta x_m \delta_m \\ &+ \sum_{n=1}^{N} W_n \Delta x_n \Delta y_n \delta_n \end{aligned} \tag{16}$$

where $\Delta y_k \Delta z_k$, $\Delta z_m \Delta x_m$ and $\Delta x_n \Delta y_n$ are surface areas facing positive or negative x-direction, y-direction and z-direction, respectively, within which the pressures are prescribed as a well boundary condition. U_k, V_m and W_n are the velocity components in x-, y- and z- directions, respectively on areas $\Delta y_k \Delta z_k$, $\Delta z_m \Delta x_m$ and $\Delta x_n \Delta y_n$, while δ_k, δ_m and δ_n are x-, y- and z- components of unit normal vector on the control surfaces, respectively, being -1 or +1.

3. PERMEABILITY MODEL

3.1 Revised AE position

In the Ogachi site, one production well and one injection well were drilled as described in detail by Hori *et al.* (1995). Though the injection well bore is sheathed by metal casing, it has two open hole intervals of $8m$ (upper: at $-705m$) and $37m$ (lower: at $-1010m$), while the production well has a long open hole interval of $400m$ reaching its deepest end ($-1100m$). The permeability coefficients of the original rock were measured before hydro-fracturing, being estimated as about $1.0 \times 10^{-16} m^2$ around the upper injection hole, and as about $3.0 \times 10^{-15} m^2$ around the lower injection hole. After high-pressure-water stimulation (fracture creation), the permeability was measured again with a pressure-response method, estimated as about $1.0 \times 10^{-14} m^2$ around the upper injection hole, and as about $1.0 \times 10^{-13} m^2$ around the lower injection hole. Kaieda *et al.* (1995) also measured positions and intensities of the acoustic emission (AE) in the Ogachi site, and revised them with more accurate velocity structure in 1999.

With the original AE data, Yamamoto *et al.* (1996) inferred spatial distribution of permeability coefficient by relating the cumulative AE magnitude (derived with Richter's law) to the local permeabil-

ity. In a similar way, the present authors defined spatial distribution of permeability with slightly different relation as shown in Fig.1 to produce the best matching with the flow rates measured in the '95 thirty-day circulation test.

Though the AE magnitude distribution was smoothed *via* spatial averaging in the original model to connect dispersed 'AE islands', it was found such smoothing is no longer needed because of the coalitional distribution of the revised AE. Such features are seen in Figs. 2 and 3 which show the original (smoothed) permeability model and the revised permeability model, respectively.

3.2 Model for Revealed Fault

Acoustic reflection measured at the Ogachi site revealed that a fault exists in SW part of Ogachi site, running in the SE-NW direction. In order to represent the fault, highest level of permeability was assigned to a plane of $20m$ (unit grid width) thickness corresponding to the fault position as shown in Fig.4.

3.3 Model for Maximum Principal Stress Orientation of Rock Mass

Geological condition and stress state measured at the Ogachi site indicate that the direction of maximum principal stress is possibly SW-NE. Based on the results, it is assumed that permeability in SW-NE direction is 1.7 times larger than those of other directions, keeping the norm of diagonal tensor of anisotropic permeability equal to that of isotropic permeability.

4. EVALUATION OF RECOVERY

A steady-state solution for 1995 Ogachi circulation test was obtained by solving eq.(10) from which the time-dependent term (left-hand-side term) was eliminated. The revised spatial distribution of permeability was used for the reservoir model. Since the temperature is not considered in the present study, density of water is set at $1000kg/m^3$ and viscosity is set at $3.0 \times 10^{-4} Pa \cdot sec.$ Pressures of $6.5MPa$ measured at the injection well head and $0.85MPa$ at the production well head corresponds to $5.3MPa$ at the injection grid and $0.95MPa$ at the production grid. With the grid pressures and zero on computational boundaries, pressure distribution was easily obtained as shown in Fig.5, where the production well is unrealistically crooked to conform to computational grids (pressure boundary conditions). Figure 6 shows streamlines originating from the two injection open holes, demonstrating preferable flow paths in the SW-NE direction due to the anisotropy of the permeability. Figure 7 shows the flow rate distribution along the open hole intervals of the injection well and the production well. The computed injection and production flow rates were $503liters/min.$ and $121liters/min.$ respectively, while the counterparts of the measurement were $500kg/min.$ and $120kg/min.$ at the quasi-steady state.

5. CONCLUSION

Permeability model used in GEOTH3D code was revised with a newly re-defined AE distribution and geological measurements of underground stress orientation and a fault near the Ogachi site. The relation between measured AE magnitude and assumed permeability was adjusted so as to reproduce a thirty-day circulation test conducted at the Ogachi in 1995.

The modified permeability model was used to evaluate water recovery assuming a new production well was drilled in the Ogachi site. The results show that the total recovery could be increased up to 44.5% if a new production well were operated with rather small back-pressure of $0.2MPa$ and if a hypothetical brick-like zone were fractured to yield highest permeability.

REFERENCES

Eguchi, Y., Yamamoto, T., Kitano, K., Nishihara, T. and Ohnishi, H., 'Three-Dimensional Computation Of Velocity And Pressure Fields in The Ogachi HDR Reservoir', 4th Int. HDR Forum, Strasbourg, FRANCE, Sept.28-30, 1998

Hori, Y., Kaieda, H and Kitano, K., 'Ogachi Project with Multi-layer Fracturing Method for HDR Geothermal Power - Outline and Future Plan - ', World Geothermal Congress Transaction, Vol.4, pp.2691-2694,1995.

Kaieda, H., Fujimitsu, Y., Yamamoto, T., Mizunaga, H. and Sasaki, S., 'AE and Mise-a-la-masse Measurements during 22-day Water Circulation Test at the Ogachi HDR Site', World Geothermal Congress Transaction, Vol.4, pp.2690-2700, 1995.

Yamamoto, T., Fujimitsu, Y. and Ohnishi, H., 'Hot Dry Rock Reservoir 3D Simulation, of the Ogachi Site', GRC Transaction Vol.19, pp.287-294, 1996.

NOMENCLATURE

L: vertical length of open hole interval $[m]$
p: pressure extracting hydrostatic pressure $[Pa]$
$p^{IN}(t)$: time-series of pressure measured at an injection well head $[Pa]$
$p^{PRO}(t)$: time-series of pressure measured at a production well head $[Pa]$

$p_{ijk}(t)$: pressure imposed at grid (i,j,k) $[Pa]$
p_{well}: pressure within a well bore $[Pa]$
$\underline{p}$: grid-averged pressure $[Pa]$
q: source or sink of mass flow per unit volume per time $[kg/m^3 \cdot sec]$
Q_0: total flow rate $[m^3/sec]$
r_w: well radius $[m]$
R: representative grid radius $[m]$

Greek letters

α: ratio of grid radius to well radius ($\alpha = \frac{R}{r_{well}}$)
β_w: compressibility coefficients for water $[Pa^{-1}]$
β_r: compressibility coefficient for rock $[Pa^{-1}]$
η: viscosity of water $[Pa \cdot sec]$

Table 1: Difference of grid-averaged pressure and well bore pressure

parameters	Inj. Well	Prod. Well
$Q_0(m^3/sec)$	-8.3×10^{-3}	$+2.1 \times 10^{-3}$
$\eta(Pa \cdot sec)$	8.5×10^{-4}	2.2×10^{-4}
$L(m)$	50	400
$k(m^2)$	1.0×10^{-13}	1.0×10^{-13}
$r_w(m)$	3.8×10^{-2}	5.2×10^{-2}
$\underline{p} - p_{well}$(MPa)	-1.2	0.10

Q_0 : Flow rate
η : Viscosity
L : Open hole length
k : Permeability
r_w : Well radius

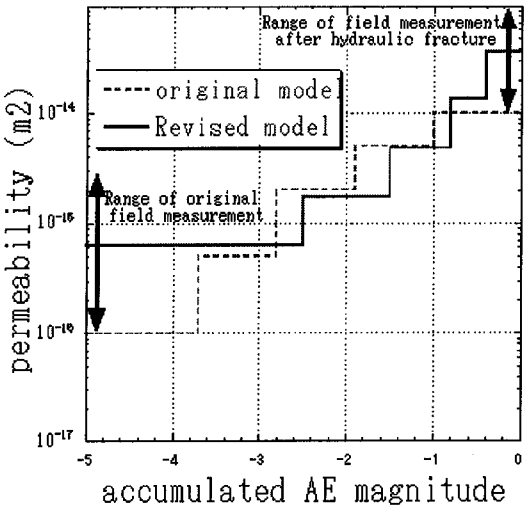

Figure 1: Relation between accumulated magnitude and assumed permeability

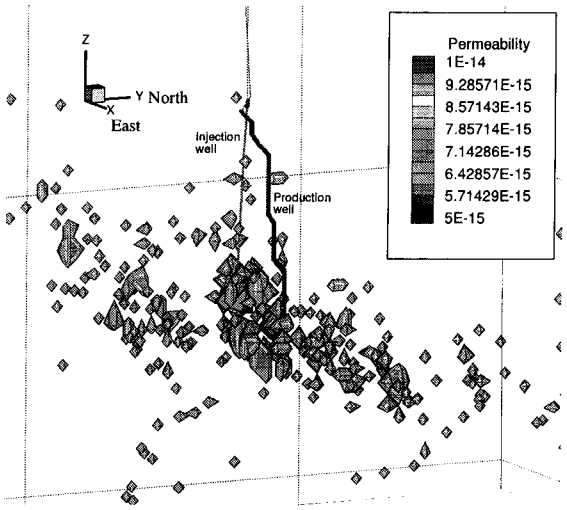

Figure 2: Permeability assumed from original AE data

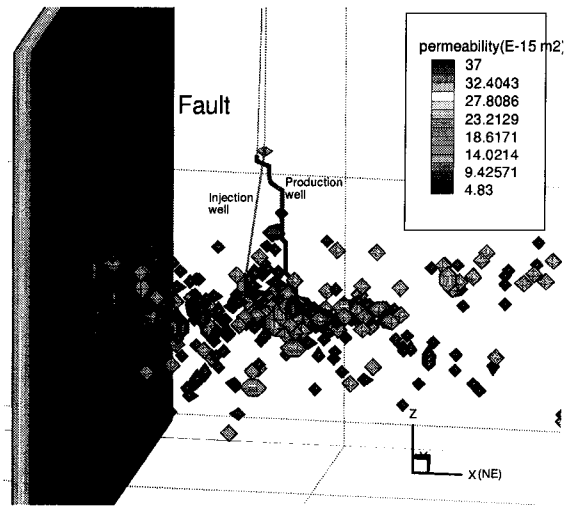

Figure 3: Permeability assumed from revised AE data

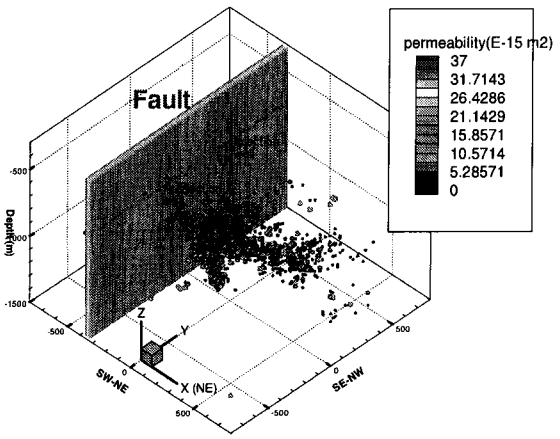

Figure 4: Overall permeability distribution including a fault model

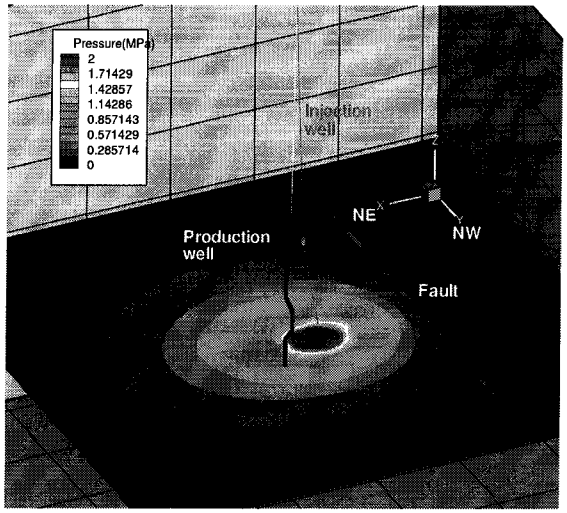

Figure 5: Computed pressure distribution for 30-day circulation test in 1995

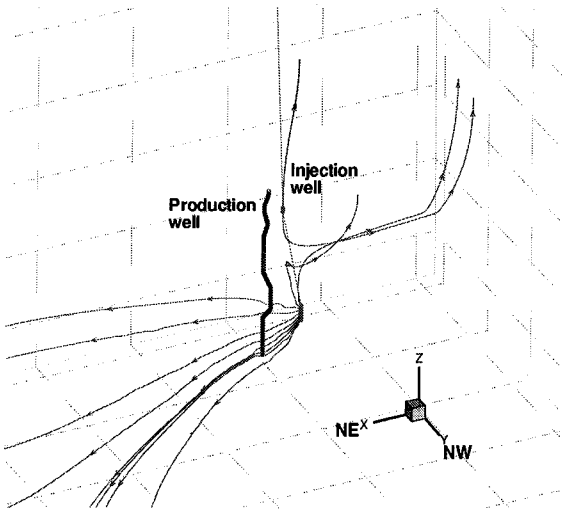

Figure 6: Computed streamlines for 30-day circulation test in 1995

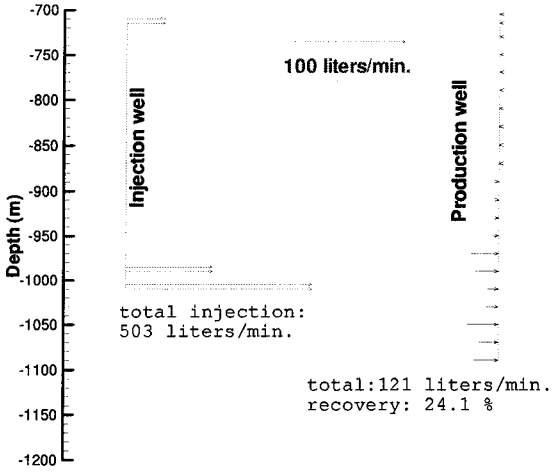

Figure 7: Flow rate distribution for 30-day circulation test in 1995